DOI: 10.15669/pnst.7.228

Progress in Nuclear Science and Technology
Volume 7 (2025) pp. 228-234

ARTICLE

Oxidation behavior of Al_4SiC_4-based ceramics at 1623K

Atsuko Tanaka [a, *], Anna Gubarevich [b], Toshiyuki Nishimura [c] and Katsumi Yoshida [b]

[a] *Department of Materials Science and Engineering, School of Materials and Chemical Technology, Tokyo Institute of Technology, 2-12-1 Ookayama, Meguro-ku, Tokyo 152-8550 Japan;* [b] *Laboratory for Zero-Carbon Energy, Institute of Innovative Research, Tokyo Institute of Technology, 2-12-1 Ookayama, Meguro-ku, Tokyo 152-8550 Japan;* [c] *Structural Non-oxide Ceramics Group, Research Center for Structural Materials, National Institute for Materials Science (NIMS), 1-1 Namiki, Tsukuba-shi, Ibaraki 305-0044 Japan*

Al_4SiC_4 is one of the nanolayered-ternary compounds with excellent properties such as oxidation and corrosion resistance at high temperatures, and we have paid attention to Al_4SiC_4 to be applied for ceramic matrix composites (CMC) as novel materials for aircraft jet engines instead of SiC. In this study, oxidation test of Al_4SiC_4-based ceramics with SiC fabricated by hot-pressing was conducted at 1623K for 12-100 h in air, and their oxidation behavior was investigated. After oxidation test, Al_4SiC_4-based ceramics had oxidation layer with a dual-layered structure in 50vol% Al_4SiC_4/50vol% SiC (Al_4SiC_4-50), four- and six-layered structure in monolithic Al_4SiC_4 (Al_4SiC_4-100), and these oxidation layers contained Al_2O_3, SiO_2 and mullite. The thickness of the oxidation layer in Al_4SiC_4-based ceramics increased with the oxidation time and the content of Al_4SiC_4, and obeyed the parabolic rate law. The schematic models of oxidation behavior of Al_4SiC_4-based ceramics with SiC were proposed based on the results of the oxidation test. In conclusions, the addition of SiC to Al_4SiC_4 enhanced the formation of mullite, which would act as the protective layer, and Al_4SiC_4-based ceramics with SiC are expected to be one of the promising materials instead of SiC.

Keywords: oxidation; Al_4SiC_4; SiC; oxidation layer

1. Introduction

Ceramics matrix composites (CMC) such as silicon carbide fiber-reinforced silicon carbide matrix (SiC_f/SiC) composites are lightweight and have excellent heat resistance, mechanical and thermal properties and thermal stability at high temperatures. CMC have been expected to be applied in the aerospace industry as hot components for aircraft jet engines [1,2]. CMC have been strongly required to withstand corrosion and oxidation in dry air and steam at high temperatures to apply for jet engines in actual environments [3,4]. We focused on the nanolayered-ternary compounds, that exhibit unique characteristics and properties of both ceramics and metals such as excellent corrosion resistance, heat resistance, thermal shock resistance and machinability [5], as novel materials for CMC. We have paid attention to Al_4SiC_4, one of the nanolayered-ternary compounds, because of its light weight, high melting point (2353K), good mechanical properties, excellent oxidation and corrosion resistance at high temperatures due to the formation mullite ($Al_6Si_2O_{13}$) and alumina (Al_2O_3) [6-9]. In addition, it has been reported that Al_4SiC_4 was used as a sintering aid for SiC and the addition of 10wt% Al_4SiC_4 to SiC achieved dense SiC by hot-pressing at 1973K [10,11].

Considering the application of CMC for aircraft jet engines, to understand the basic oxidation behavior of Al_4SiC_4-based ceramics in dry air at high temperatures becomes one of the important studies. Although the oxidation behavior of each monolithic SiC and Al_4SiC_4 at high temperatures has been studied [12-14], there are few reports on the oxidation behavior of Al_4SiC_4-based ceramics with SiC at high temperatures in dry air. Moreover, there has been no report regarding the fabrication of Al_4SiC_4/SiC ceramics with changing their composition and their oxidation behavior at high temperatures in air. In order to understand the basic properties of Al_4SiC_4/SiC ceramics, we have fabricated Al_4SiC_4-based ceramics with SiC and investigated their corrosion behavior against calcium-magnesium-alumino-silicate (CMAS) at 1623K in Ar [15]. Test temperature (1623K) for corrosion test was determined by considering the expected operation temperature (material surface temperature) for hot components of aircraft jet engines in the range of 1573-1673K [16]. In this study, Al_4SiC_4-based ceramics with SiC were fabricated by hot-pressing, and oxidation test was conducted at 1623K for 12-100 h in dry air, and their oxidation behavior was investigated.

*Corresponding author. E-mail: tanaka.ac.18@gmail.com

2. Experimental procedure

2.1. Preparation of Al_4SiC_4-based ceramics by hot-pressing

Al_4SiC_4 powder (D_{50}: 3.3 μm, Tateho Chemical Industries Co., Ltd., Japan) and β-SiC powder (D_{50}: 0.5 μm, Höganäs, Sweden) were used as starting materials. These powders were weighed as the volume ratio of Al_4SiC_4:SiC was 100:0 (denoted as Al_4SiC_4-100), 90:10 (Al_4SiC_4-90), 50:50 (Al_4SiC_4-50), and 10:90 (Al_4SiC_4-10). The starting powder was mixed by wet ball-milling for 24 h. The mixed powder was formed into the compact, and then hot-pressed at 2073K for 2 h in Ar at mechanical pressure of 40 MPa. For comparison, commercially available α-SiC (Kyocera Corporation, Japan; SiC-100) was used. Their bulk density and open porosity were measured by Archimedes' method. **Table 1** shows their relative density and open porosity. Theoretical density of Al_4SiC_4 and SiC was assumed to be 3.03 g/cm^3 [7] and 3.21 g/cm^3 [17], respectively to calculate the relative density. Except for Al_4SiC_4-10, their open porosity was less than 0.4%, and their relative density was over 90%, and the dense samples were achieved.

2.2. Oxidation test and characterization

The hot-pressed Al_4SiC_4-based ceramics were cut into the plates with the size of 15 x 7.5 x 3 mm^3, and their surface was mirror-polished. The sample was put on a mullite plate in an Al_2O_3 crucible, and then placed in an air furnace. The oxidation test was conducted at 1623K for 12, 24 and 100 h in air. The weight change of the samples before and after the oxidation test was measured with an electronic balance. The surface of the oxidized samples was covered with a thin glass plate using resin. They were cut into pieces and their cross-section was mirror-polished. The mirror-polished surface was observed with scanning electron microscope (JSM-7000, JEOL Ltd., Japan) equipped with energy dispersive X-ray spectroscope (EDS) to measure the thickness of reaction layer of the samples after oxidation test and to analyze the element distribution of the oxidized samples. In addition, the crystalline phases of the samples at the surfaces after oxidation test were analyzed by X-ray diffractometry (Aeris, Malvern Panalytical Ltd., UK).

3. Results

3.1. Reaction products of Al_4SiC_4-based ceramics after oxidation test analyzed by XRD

Figure 1 shows XRD patterns of the samples after oxidation test at 1623K for 12-100 h and the starting materials. For SiC-100, cristobalite (SiO_2) was formed after oxidation, and the peak intensities for SiO_2 after

Table 1. Volume ratio of starting materials, the relative density and open porosity of the samples, and change in thickness of the oxidation layer with oxidation time.

Sample name	Al_4SiC_4 (vol %)	SiC (vol %)	Relative density (%)	Open porosity (%)	Thickness oxidation layer (μm)		
					Oxidation time		
					12 h	24 h	100 h
Al_4SiC_4-100	100	0	91.0	0.30	20	28	42 (37-47)*
Al_4SiC_4-90	90	10	94.3	0.30	15	18	38
Al_4SiC_4-50	50	50	93.2	0.38	10	13	24
Al_4SiC_4-10	10	90	87.4	3.91	0.7	0.5	0.8
SiC-100	0	100	98.4	0.16	0.6	0.6	1.0

*These values were the thickness of the oxidation layers with four- and six-layered structures, respectively.

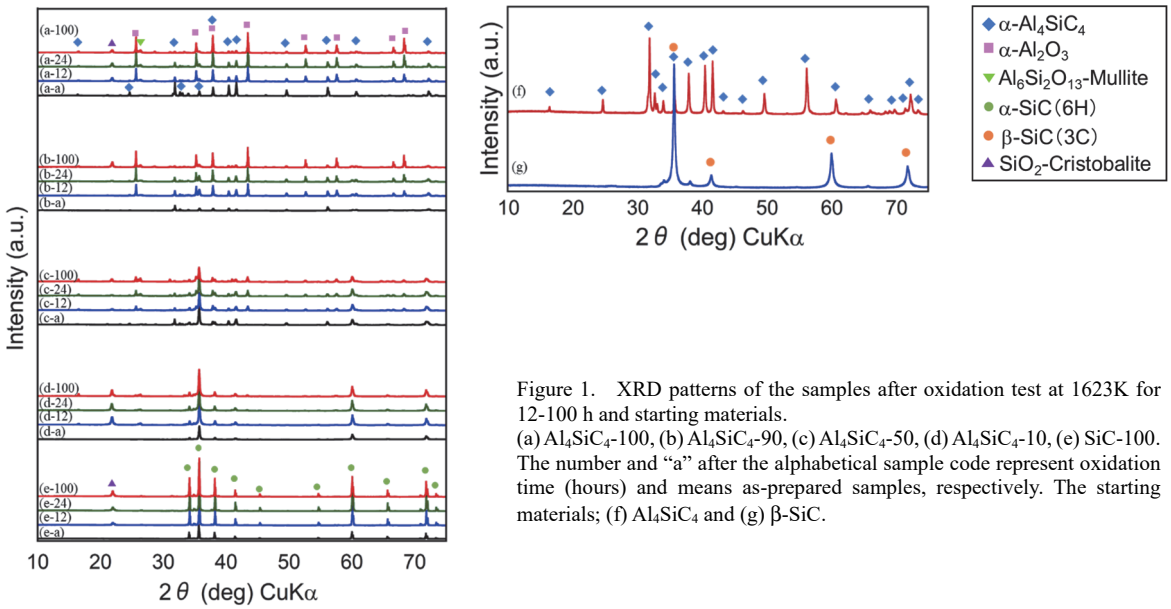

Figure 1. XRD patterns of the samples after oxidation test at 1623K for 12-100 h and starting materials.
(a) Al_4SiC_4-100, (b) Al_4SiC_4-90, (c) Al_4SiC_4-50, (d) Al_4SiC_4-10, (e) SiC-100. The number and "a" after the alphabetical sample code represent oxidation time (hours) and means as-prepared samples, respectively. The starting materials; (f) Al_4SiC_4 and (g) β-SiC.

oxidation for 100 h became slightly higher than those after oxidation for 12 and 24 h. In the case of Al_4SiC_4-100, α-Al_2O_3, SiO_2 and mullite were formed after oxidation, and the peak intensities for Al_2O_3 and mullite after oxidation for 100 h much increased. Al_4SiC_4-based ceramics after oxidation contained Al_2O_3, SiO_2 and mullite. The XRD results confirmed the amount of these products depended on the composition of Al_4SiC_4-based ceramics. For Al_4SiC_4-90, Al_4SiC_4 decreased but Al_2O_3 and mullite increased with oxidation time. After oxidation for 100 h, SiC decreased significantly, resulting in an increase in SiO_2. For Al_4SiC_4-10, diffraction peaks for Al_4SiC_4 almost disappeared after oxidation for 12 h, and the peaks for mullite appeared. Whereas SiO_2 decreased after oxidation for 100 h, Al_2O_3 and mullite increased. For Al_4SiC_4-50, mullite increased with oxidation time although the amount of Al_2O_3 and SiO_2 did not change with oxidation time. In addition, Al_4SiC_4 and SiC decreased after oxidation for 100 h.

3.2. Microstructure of oxidation layers after oxidation test evaluated by SEM

The cross-sectional SEM images of the samples after oxidation test at 1623K for 12-100 h were exhibited in **Figure 2.** All the samples had reaction layers formed by oxidation reaction at their surface (oxidation layer). The oxidation layers of Al_4SiC_4-50, -90 and -100 became thicker as the oxidation time increased, and these oxidation layers consisted of porous and dense layers. Al_4SiC_4-50 after oxidation had dual oxidation layers consisting of porous and dense layers.

The number of oxidation layers in Al_4SiC_4-90 and Al_4SiC_4-100 increased from two to four and from four to six with oxidation time, respectively. For Al_4SiC_4-10 and SiC-100, the thickness of oxidation layers was very thin. Whereas the oxidation surface of SiC-100 was flat, that of Al_4SiC_4-10 and -50 was partially rough.

3.3. The change in the weight and the thickness of oxidation layer of Al_4SiC_4-based ceramics with oxidation time

Figure 3 shows the weight change of the samples after oxidation test at 1623K for 12-100 h. Except for Al_4SiC_4-10, the weight of the samples increased with oxidation time, and their weight change became larger as Al_4SiC_4 content increased. This weight change behavior followed the parabolic rate law expressed as equation (1) [7] except for Al_4SiC_4-10 and SiC-100, and rate-controlling step in the oxidation reaction is considered to be the diffusion reaction;

$$(\Delta W)^2 = k_p t \quad (1)$$

where ΔW is weight change per surface area of the sample, t oxidation time, and k_p parabolic rate constant. It has been reported that the oxidation reaction of monolithic SiC obeys the parabolic rate law [18]. In this study, however, it was unclear whether the oxidation behavior of SiC-100 agreed with the parabolic rate law under the present experimental condition or not. On the contrary, the weight of Al_4SiC_4-10 after oxidation for 24 h decreased from the initial weight, and its weight after oxidation for 100 h increased almost to the initial weight.

Table 1 lists the average thickness of the oxidation layer of the samples measured from SEM images, and these values are plotted in **Figure 4**. For Al_4SiC_4-50, -90 and -100, their thickness of oxidation layers increased with the oxidation time and the content of Al_4SiC_4. The thickness of oxidation layer in Al_4SiC_4-100 became approximately twice from 20 to 40 μm as the oxidation time changed from 12 to 100 h. The thickness of oxidation layers in Al_4SiC_4-50 and -90 after oxidation for 100 h was about 24 μm and 38 μm, respectively. The change in the thickness of oxidation layer also followed the parabolic rate law expressed as equation (2) [19] as well as the weight change behavior;

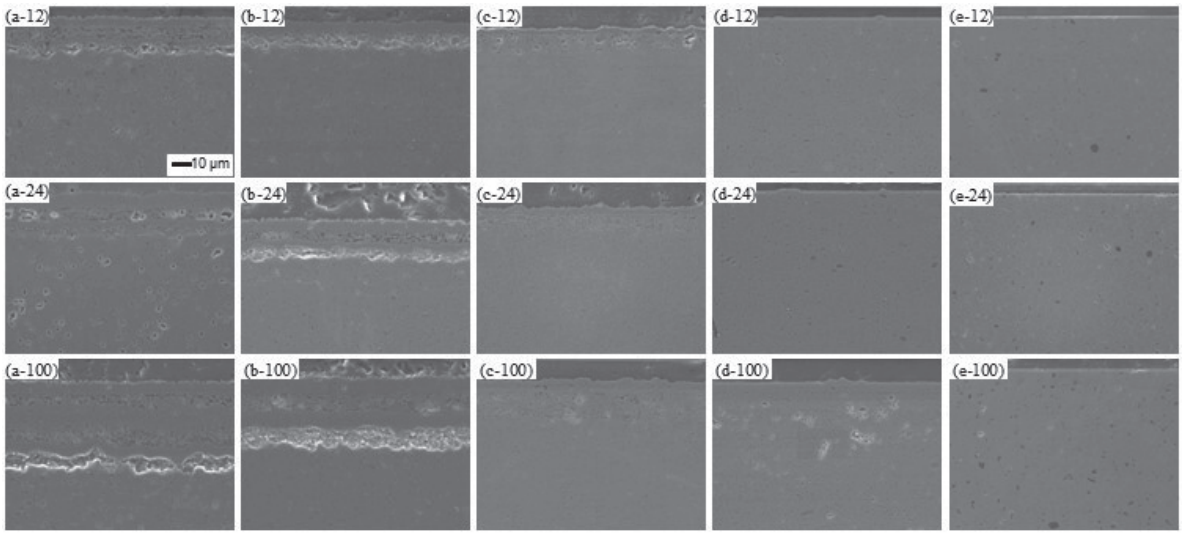

Figure 2. Cross-sectional SEM images of the samples after oxidation test at 1623K for 12-100 h.
(a) Al_4SiC_4-100, (b) Al_4SiC_4-90, (c) Al_4SiC_4-50, (d) Al_4SiC_4-10, (e) SiC-100. The number after the alphabetical sample code represents oxidation time (hours).

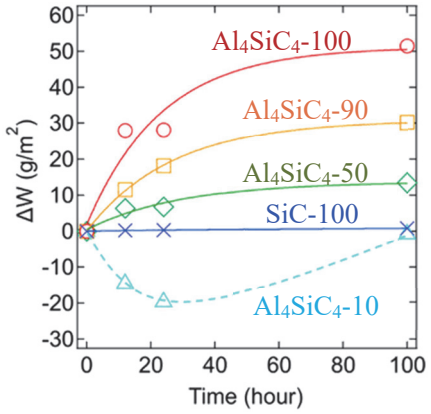

Figure 3. Weight change of the samples after oxidation test at 1623K for 12-100 h.

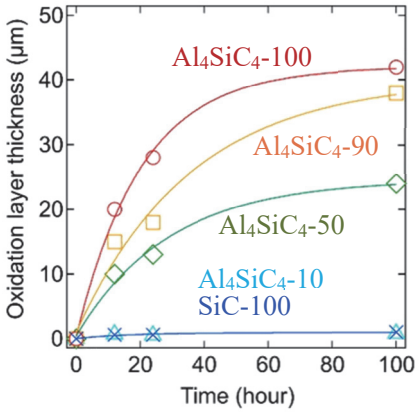

Figure 4. Oxidation layer thickness of the samples after oxidation test at 1623K for 12-100 h.

$$x^2 = k_p t \tag{2}$$

where x is the thickness of oxidation layer of the sample. The thickness of the SiC-rich samples (SiC-100 and Al_4SiC_4-10) was less than 1 μm and did not change with oxidation time.

3.4. EDS mapping of the cross-section of the samples after oxidation test

Figure 5 shows EDS mapping of the cross section of the samples after oxidation test. For SiC-100 after oxidation for 12 h, Si and O were detected at its surface to the depth of around 1 μm, and this layer was considered to be SiO_2. SiC-100 after oxidation for 24 and 100 h showed almost the same element distribution as oxidation for 12 h. Al_4SiC_4-100 after oxidation for 12 and 24 h had four-layered structure, and both four- and six-layered structures were observed after oxidation for 100 h. The four-layered structure had alternate layers with higher concentration of Al and O (Al/O layer), with Si, C, O and small amount of Al (Si/O/C/(Al) layer), with Al, O and small amount of Si (Al/O/(Si)) and with Si, O, C and small amount of Al (Si/O/C/(Al)) (Figure 5(a-100-1)). On the other hand, the six-layered region consisted of Al/O, Si/O/C/(Al), Al/O/(Si), Si/O/C/(Al), Al/O/(Si) and Si/O/C/(Al) layers (Figure 5 (a-100-2)). In addition, the six-layered structure was thicker than the four-layered structure in the Al_4SiC_4-100 after oxidation for 100 h. The oxidation layer of Al_4SiC_4-90 after oxidation for 12 h was dual-layered structure; one layer with concentrated Al/O, and another with Si/O/C/(Al). The Al_4SiC_4-90 after oxidation for 24 h had not only dual-layered but also four-layered structures as the oxidation layer, and the oxidation layer after oxidation for 100 h was four-layered structure as the same as Al_4SiC_4-100. The thickness of each layer in dual- or four-layered structure increased with the oxidation time. In Al_4SiC_4-50 had a dual-layer consisting of the upper layer with Al/O and the lower layer with Si/O/C/(Al). In the Si/O/C/(Al) layer, lower layer of the dual-layer, the concentration of C became higher in the lower region whereas the concentration Al and O gradually decreased from the upper to lower region in this layer. EDS mapping also revealed that the thickness of the oxidation layer increased with the oxidation time. While Si and C existed entirely in Al_4SiC_4-10, Al was detected partially. This result showed that Al_4SiC_4 partially existed in Al_4SiC_4-10. The thickness of the O-rich layer in the Al_4SiC_4-10 after oxidation for 12-100 h was almost the same as that in the SiC-100, but this layer contained not only Si, O but Al, and Al-rich layer was clearly observed in the Al_4SiC_4-10 after oxidation for 100 h.

4. Discussion

Figure 6 shows the schematic models of oxidation behavior of Al_4SiC_4-100, -50 and SiC-100. The Gibbs energy at 1623K for each reaction were calculated based on the thermodynamic databases (MALT and Fact Web).

SiC are known to be passively oxidized in air (high oxygen partial pressure) at high temperatures expressed as the following reaction [3];

$$SiC\,(s) + 3/2\,O_2\,(g) \rightarrow SiO_2\,(s) + CO\,(g) \tag{3}$$
$$\Delta G^0_{1623K} = -828.357\ (kJ/mol)$$

In this study, passive oxidation occurred in SiC-100, and SiO_2 (cristobalite) was formed. It is reported that SiO_2 formed by passive oxidation acts as a protective layer against the oxidation [20], and our results agreed with this oxidation behavior.

The oxidation reaction of Al_4SiC_4-100 would occur according to the reactions (4) [12] and (5) [14], and Al_2O_3 and SiC were formed. Furthermore, the SiC was also oxidized as SiO_2 according to the reaction (3). These oxides would form mullite according to the reaction (6) [14];

$$Al_4SiC_4\,(s) + 6O_2\,(g) \rightarrow 2Al_2O_3\,(s) + SiC\,(s) + 3CO_2\,(g) \tag{4}$$
$$\Delta G^0_{1623K} = -3473.165\ (kJ/mol)$$

$$Al_4SiC_4\,(s) + 3O_2\,(g) \rightarrow 2Al_2O_3\,(s) + SiC\,(s) + 3C\,(s) \tag{5}$$
$$\Delta G^0_{1623K} = -2283.449\ (kJ/mol)$$

$$3Al_2O_3\,(s) + 2SiO_2\,(s) \rightarrow Al_6Si_2O_{13}\,(s) \qquad (6)$$
$$\Delta G^0_{1623K} = -24.654\ (kJ/mol)$$

The change in the weight of the samples and the thickness of the oxidation layer increased with oxidation time, but their change became small after the oxidation time of 24 h, and it obeyed the parabolic rate law. This result suggested that the Al_2O_3, SiO_2 and mullite would act as the protective layers against oxidation. The oxidation mechanism of Al_4SiC_4-100 can be proposed as shown in

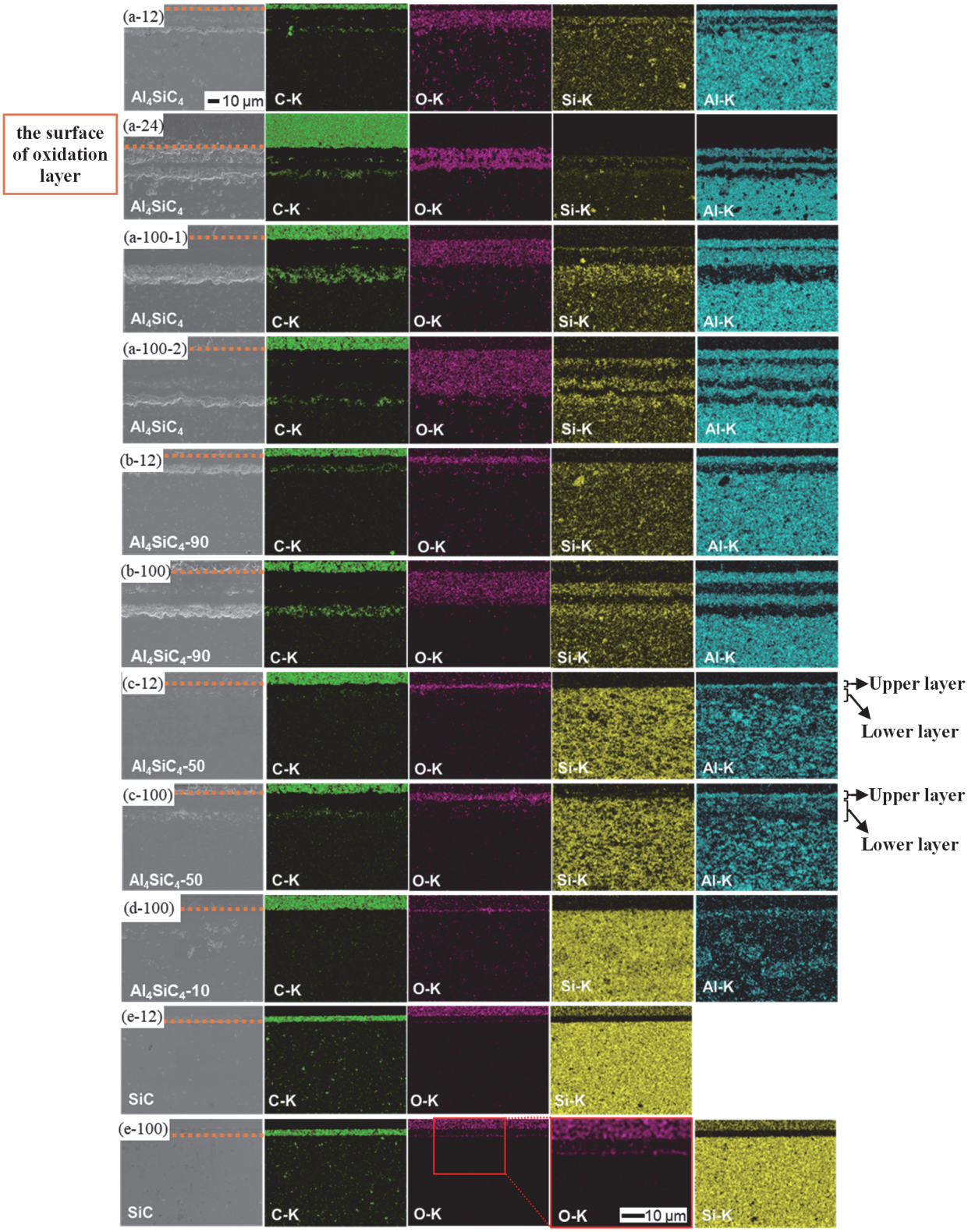

Figure 5. EDS mapping of the cross-section of the samples after oxidation test at 1623K for 12-100 h.
(a) Al_4SiC_4-100, (b) Al_4SiC_4-90, (c) Al_4SiC_4-50, (d) Al_4SiC_4-10, (e) SiC-100.
The number after the alphabetical sample code represents oxidation time (hours).

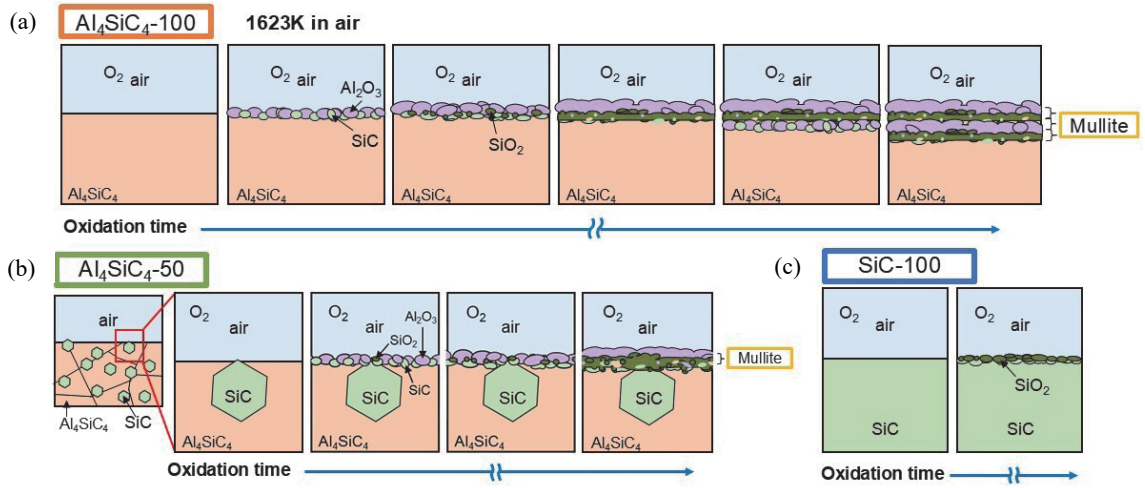

Figure 6. The schematic models of oxidation behavior of (a) Al_4SiC_4-100 and (b) -50, (c) SiC-100.

Figure 6(a); in the early stage, Al_2O_3 and SiC were formed, followed by the formation of SiO_2, and it reacted with Al_2O_3, resulting in the formation of mullite. As oxidation time extends, oxygen diffuses inward the sample and further oxidation proceeds at the interface between the oxidation layer and Al_4SiC_4, and the oxidation reactions occur repeatedly. As the number of layers increases by oxidation, these layers, i.e. mullite, Al_2O_3 and SiO_2 act as the protective layers against the oxidation and they inhibit the diffusion of oxygen, resulting in lower oxidation rate. The thickness of the oxidation layer would be saturated as the oxidation time increased under the present oxidation condition. In the case of Al_4SiC_4-50, both oxidation of SiC and Al_4SiC_4 occurred. The layer formed by the oxidation of Al_4SiC_4 was thicker than that formed by the oxidation of SiC. Furthermore, Al_4SiC_4 had much larger grain size than SiC. As a result, Al_2O_3 layer was formed on the whole surface of the sample. Not only SiC formed by oxidation of Al_4SiC_4 but also SiC initially existed in the sample were oxidized to form SiO_2, which reacted with Al_2O_3, and then mullite was formed at the interface between SiO_2 and Al_2O_3. Since these oxides act as the protective layers for Al_4SiC_4 against oxidation, Al_4SiC_4 would still exist in the layer containing SiO_2 and SiC. Al_4SiC_4-90 had the oxidation layer with almost the same structure as Al_4SiC_4-100. SiC in Al_4SiC_4-90 was oxidized as SiO_2, and it enhanced the formation of mullite rather than Al_4SiC_4-100. As a result, the mullite would act as the protective layer against oxidation, and thus the thickness of the oxidation layer was thinner than that of Al_4SiC_4-100.

Al_4SiC_4-10 had SiO_2 layer on its surface as well as SiC-100. XRD patterns suggested that the oxidation of SiC and Al_4SiC_4 occurred, and Al_2O_3, SiO_2 and mullite were formed, i.e., these oxides were considered to partially exist because Al_4SiC_4-10 contains 90vol% SiC, and Al_4SiC_4 was partially distributed inside the sample. The oxidation of SiC was dominant in Al_4SiC_4-10, and the thickness of the oxidation layer in Al_4SiC_4-10 was almost the same as that in SiC-100. On the other hand, the weight loss of Al_4SiC_4-10 took place up to the oxidation time of 24 h. The volume change was larger for Al_4SiC_4-50, -90 and -100, and smaller for Al_4SiC_4-10. The density change was negatively larger for Al_4SiC_4-10 than for Al_4SiC_4-50, -90 and -100. This means that the weight loss by oxidation was dominant in Al_4SiC_4-10. The weight loss occurred in Al_4SiC_4-10 by oxidation was caused by promoting the oxidation of Al_4SiC_4 by CO formed by the oxidation of SiC expressed as reaction (7) [21]. Although this reaction would occur for all the samples containing Al_4SiC_4, the content of SiC in Al_4SiC_4 probably affects the promotion of this reaction, i.e. higher SiC content like Al_4SiC_4-10 could enhance this reaction. The oxidation of SiC produced in the reaction (7) also formed CO, and the CO would further promote the reaction (7). In addition, C formed by the reaction between Al_4SiC_4 and CO was oxidized to CO or CO_2, the oxidation of C would cause the weight loss of Al_4SiC_4-10. When this reaction proceeded, the oxidation of SiC would be dominant, and thus the weight gain occurred. Another reason why this weight gain occurred after oxidation test for 100 h was that the weight loss related to reaction (7) would be suppressed because Al_2O_3 and SiO_2 formed by the oxidation of Al_4SiC_4 and SiC, respectively, acted as the protective layer and CO produced by the oxidation of C was reduced.

$$Al_4SiC_4\,(s) + 6CO\,(g) \rightarrow 2Al_2O_3\,(s) + SiC\,(s) + 9C\,(s) \quad (7)$$
$$\Delta G^0_{1623K} = -757.435\ (kJ/mol)$$

In conclusions, the addition of SiC to Al_4SiC_4 enhanced the formation of mullite, which would act as the protective layer, and Al_4SiC_4-based ceramics with SiC are expected to be one of the promising materials instead of SiC.

5. Conclusion

Oxidation test of Al_4SiC_4 and Al_4SiC_4/SiC ceramics was conducted at 1623K for 12-100 h in air, and their oxidation behavior was investigated. The oxidation layer

formed in Al_4SiC_4-based ceramics with SiC after oxidation contained Al_2O_3, SiO_2, and mullite. The thickness of the oxidation layer increased with the oxidation time and the content of Al_4SiC_4, and obeyed the parabolic rate law. The schematic models of the oxidation behavior of Al_4SiC_4-100, -50 and SiC-100 were proposed based on the results. Whereas SiC-100 had SiO_2 layer as oxidation layer, Al_4SiC_4-based ceramics with SiC had complicated oxidation layers such as dual-, four- and six-layered structures. These oxidation layers observed in Al_4SiC_4-based ceramics with SiC act as the protective layers against oxidation. The addition of SiC to Al_4SiC_4 enhanced the formation of mullite, which would act as the protective layer. It is concluded that Al_4SiC_4-based ceramics with SiC are expected to be one of the promising materials instead of SiC.

Acknowledgements

The authors would like to deeply appreciate Dr. Shintaro Yasui and Dr. Ayumi Itoh (Tokyo Institute of Technology) for their kind support for conducting SEM observation and EDS analysis.

References

[1] H. Kaya, The application of ceramic–matrix composites to the automotive ceramic gas turbine, *Compos. Sci. Technol.*, 59 (1999), pp. 861-872.

[2] L. Giancarli, G. Aiello, A. Caso, A. Gasse, G. Le Marois, Y. Poitevin, J.F. Salavy and J. Szczepanski, R&D issues for SiC_f/SiC composites structural material infusion power reactor blankets, *Fusion Eng. Des.*, 48 (2000), pp. 509-520.

[3] K.N. Lee, Chapter 15, Environmental barrier coatings for SiC_f/SiC, Bansal, N. P., and Lamon, J. eds., *Ceramic Matrix Composites: Materials, Modeling and Technology, First Edition* (2015), pp.430-451, John Wiley & Sons, Inc., USA.

[4] M. Tanaka, S. Kitaoka, M. Yoshida, O. Sakurada, M. Hasegawa, K. Nishioka and Y. Kagawa, Structural stabilization of EBC with thermal energy reflection at high temperatures, *J. Euro. Ceram. Soc.*, 37 (2017), pp. 4155-4161.

[5] Y. Zhou and Z. Sun, Electronic structure and bonding properties in layered ternary carbide Ti_3SiC_2, *J. Phys.*, 12 (2000), pp. L457-L462.

[6] K. Inoue and A. Yamaguchi, Synthesis of Al_4SiC_4, *J. Am. Ceram. Soc.*, 86 (2003), pp. 1028-1030.

[7] X.X. Huang, G.W. Wen, X.M. Cheng and B.Y. Zhang, Oxidation behavior of Al_4SiC_4 ceramic up to 1700 °C, *Corros. Sci.*, 49 (2007), pp. 2059-2070.

[8] V.A.Gubarevich, T.Watanabe, T. Nishimura and K. Yoshida, Combustion synthesis of single-phase Al_4SiC_4 powder with assistance of induction heating, *J. Am. Ceram. Soc.*, 103 (2020), pp. 744-749.

[9] R. Wills and S. Goodrich, The Oxidation of Aluminum Silicon Carbide, *Ceram. Eng. Sci. Proc*. 26 (2005), pp. 181-188.

[10] J.S. Lee, S.H. Lee, T. Nishimura, N., Hirosaki and H. Tanaka, A ternary compound additive for vacuum densification of β-silicon carbide at low temperature, *J. Euro. Ceram. Soc*. 29 (2009), pp. 3419-3423.

[11] J.S. Lee, Y.S. Ahn, T. Nishimura, H. Tanaka S.H. Lee, Effect of Al_4SiC_4 additive on the densification of β-silicon carbide under vacuum, *J. Euro. Ceram. Soc*. 32 (2012), pp. 619-625.

[12] A. Yamaguchi and S. Zhang, Synthesis and Some Properties of Al_4SiC_4, *J. Ceram. Soc. Japan*, 103 (1995), pp. 20-24.

[13] T. Narushima, T. Goto, T. Hirai and Y. Iguchi, High-Temperature Oxidation of Silicon Carbide and Silicon Nitride, *Mater. Trans., JIM* 38 (1997), pp. 821-835.

[14] K. Inoue, A. Yamaguchi and S. Hashimoto, Fabrication and Oxidation Resistance of Al_4SiC_4 Body, *J. Ceram. Soc. Japan*, 110 (2002), pp. 1010-1015 [in Japanese].

[15] A. Tanaka, V.A. Gubarevich, T. Nishimura and K. Yoshida, Corrosion behavior of Al_4SiC_4-based ceramics with molten CMAS at 1350°C in Ar, *Proc. JSME International Conference on Materials and Processing* 2022 (2022), Mo-2B-2.

[16] K. Yoshida, Recent Development on Ceramics-Based Continuous Fiber-Reinforced Composites, Bull. Ceram. Soc. Japan, 50 (2015), pp. 469-473 [in Japanese].

[17] F.L. Riley, Silicon carbide, *Structural Ceramics Fundamentals and Case Studies* (2009), pp. 175-245, Cambridge University Press, NY, USA.

[18] J.A. Costello and R.E. Tressler, Oxidation Kinetics of Hot-Pressed and Sintered α-SiC, *J. Am. Ceram. Soc*. 64 (1981), pp. 327-331.

[19] P. Goursat and S. Foucaud, Chapter 7 Non-oxide Ceramics, Ceramic Materials: *Processes, Properties, and Applications*, in ; Boch, R., Niepce, J. C. (Eds.), (2007), pp. 249-252, ISTE Ltd., UK.

[20] B. Chayasombat, T. Kato, T. Hirayama, T. Tokunaga, K. Sasaki and K. Kuroda, Characterization of microstructures of thermal oxide scales on silicon carbide using transmission electron microscopy, *J. Ceram. Soc. Japan* 120 (2012), pp. 64-68.

[21] S. Zhang and A. Yamaguchi, Effect of Al_4SiC_4 Addition to Carbon-Containing Refractories, *J. Ceram. Soc. Japan* 103 (1995), pp.235-239.